

Performance-based evaluation of strap-braced cold-formed steel frames using incremental dynamic analysis

M.R. Davani, S. Hatami* and A. Zare

Department of Civil Engineering, Yasouj University, Yasouj, Iran

(Received July 15, 2015, Revised August 18, 2016, Accepted August 22, 2016)

Abstract. This study is an effort to clearly recognize the seismic damages occurred in strap-braced cold formed steel frames. In order to serve this purpose, a detailed investigation was conducted on 9 full scale strap-braced CFS walls and the required data were derived from the results of the experiments. As a consequence, quantitative and qualitative damage indices have been proposed in three seismic performance levels. Moreover, in order to assess seismic performance of the strap-braced CFS frames, a total of 8 models categorized into three types are utilized. Based on the experimental results, structural characteristics are calculated and all frames have been modeled as single degree of freedom systems. Incremental dynamic analysis using OPENSEES software is utilized to calculate seismic demand of the strap-braced CFS walls. Finally, fragility curves are calculated based on three damage limit states proposed by this paper. The results showed that the use of cladding and other elements, which contribute positively to the lateral stiffness and strength, increase the efficiency of strap-braced CFS walls in seismic events.

Keywords: performance-based; cold formed steel frame; strap braced; seismic; incremental dynamic analysis (IDA); fragility curve

1. Introduction

Although seismic provisions have made very significant advances in anticipation of seismic behavior of buildings, performance evaluation of structures against earthquake excitations is still a great challenge as a result of wide range of the uncertainty of demand and capacity of structures which they result from the probabilistic nature of earthquake excitation, such as source, frequency, content, intensity, direction of ground motions, and structural properties in both design and construction.

The seismic probabilistic analysis methodology is the most commonly approach for the evaluation of seismic performance of structures. It seems that probabilistic analysis can be very helpful in assessing the seismic performance of the structures. In this framework, fragility curves express the conditional probability of exceeding of a structural response, such as maximum inter-story drift from prescribed limit state (a certain seismic performance level) for a given seismic earthquake excitation parameter, such as peak ground acceleration (PGA). In recent years, researchers have used the fragility curves to evaluate seismic performance of several types of

*Corresponding author, Ph.D., E-mail: hatami@yu.ac.ir

buildings (Kiani *et al.* 2016, Khaloo *et al.* 2016, Ghowsi and Sahoo 2015, Karantoni *et al.* 2014).

Cold Formed Steel (CFS) buildings are vastly widespread in use over the recent decade, which results in hard struggles by seismic provisions to assess seismic behavior of CFS structures characterized by the lateral response of shear walls, such as sheathed-braced walls, knee-braced walls, K-braced walls, and one of the most popular lateral resistance systems, the strap-braced CFS wall. A strap-braced stud wall is comprised of chord and framing studs, top and bottom tracks, diagonal strap braces and their connections, and anchorage system includes hold-downs, anchor bolts, and fasteners. These elements are designed to be able to transfer the gravity and the lateral loads to foundation. In recent years, many experimental investigations have been conducted to assess the seismic behavior of strap-braced CFS structures. Kim *et al.* (2006) investigated non-linear dynamic behavior of the CFS shear panels by the shaketable test of a full-scale two-story one-bay structure. In this test, a number of beneficial results such as effective role of thin strap as a ductile member and the positive contribution of the columns to the shear capacity are observed. Casafont *et al.* (2006a, b) carried out extensive step by step tests on screwed joints in straps, bolted joints in straps. Also, they conducted a series of tests in gussets, corner joints and x-braced frames in order to recognize all modes of failure of a strap-braced stud wall and to attain a perfect seismic performance of these walls (Casafont *et al.* 2007). Al-kharat and Rogers (2007) tested sixteen strap-braced stud walls categorized in three types based on their lateral resistance. They calculated the response modification factor of these walls and compared with those values of the seismic code. Fulop and Dubina (2008) used six series of full-scale walls with different cladding in order to investigate seismic performance of these walls under lateral loads. Moghimi and Ronagh (2009a) conducted their experiments on light strap-braced stud walls categorized in five types where the aspect ratio, the size of the straps, cladding and use of the brackets were the distinct differences. In order to investigate the role of corner brackets on lateral resistance more precisely, Moghimi and Ronagh (2009b) conducted a series of experiments on strap-braced CFS stud walls with and without the brackets. Velchev *et al.* (2010) evaluated the lateral resistance of typical welded and screw-connected single-story strap braced walls using 44 X-braced walls with aspect ratios from 4:1 to 1:1. The results of these experiments represented a large number of damages such as local and distortional buckling of studs, bearing of studs and tracks, tearing in the flange of stud or track in the fasteners location, tilting and pulling out of the fasteners, and strap yielding. Iourio *et al.* (2014) investigated seismic response of CFS strap-braced stud walls by twelve specimens categorized to three types under monotonic and cyclic load. They also recognized some probable modes of failure of these walls. Accordingly, various damages can be identified and they can be classified at different levels depending on their effects on the seismic performance of the walls.

In this study, quantitative and qualitative damage indices were proposed by recognizing the damage modes using full scale strap-braced CFS stud walls. The effects of these damages on lateral resistance are closely investigated and the seismic performance levels were obtained for strap-braced CFS walls. In order to assess the seismic performance of the strap-braced CFS walls and predict how a strap-braced wall respond to seismic events, the fragility curves have been derived from Incremental Dynamic Analysis (IDA) outcomes. Finally, considering that every seismic code has a specific performance objective which anticipates considerable damages after seismic events, the fragility curves have been used to evaluate the wall's conditions after different earthquakes and compare them with the performance objective of the code. In other words, this methodology revealed that how this structural system reacts against different ground motions which may be experienced during their life.

2. Code provisions

Seismic codes limit the story drift of the structures based on their general structural properties and seismic area. However, they have not categorized structural systems according to their drift limitations. In other words, these codes have placed different structural systems into overall categories and limit their lateral displacement in order to achieve a specific performance objective. Some of these code provisions are reviewed below.

2.1 FEMA 450

The performance objectives of the *NEHRP Recommended Provisions for Seismic Regulations for New Buildings and Other Structures* (FEMA 450) are as follows: 1. Providing the safety and health of the general public by minimizing the seismic hazard risk to life and 2. Improving immediate function of essential facilities and structures containing substantial quantities of hazardous materials during and after design earthquakes.

According to these Provisions, structural and nonstructural damages after the design earthquake ground motion are undeniable; however, it would be repairable. Also, essential facilities are expected to maintain their stability with no considerable damage to both structural and nonstructural elements. Finally, for ground motions larger than the design earthquake, it is expected to be a low likelihood of structural collapse.

FEMA 450 limits the story drift ratio to 2.5%, 2.0% and 1.5% for seismic use group I, II and III, respectively, for structures lower or equal four stories including interior walls, partitions ceilings, and exterior wall systems.

2.2 FEMA 356

According to *NEHRP guidelines for the seismic rehabilitation of buildings* (FEMA 356), “the important limit states of light frame shear walls are considered as sheathing failure, connection failure, tie-down failure, and excessive deflection which define the point of life safety and, often, of structural stability.” The Immediate Occupancy (IO) level is defined as the point of yielding displacement calculating with the aid of bilinear force-displacement curve of the wall. In order to characterize the seismic performance levels of strap-braced CFS walls, FEMA 356 has referred to acceptance criteria of custom steel structures.

2.3 ASCE07-10

The first basic performance objective in ASCE07-10 is that structures will have low probability of failure in the maximum considered earthquake (MCE) ground motion. ASCE07-10 considers maximum probability of total or partial structural collapse conditioned on the occurrence of MCE ground motion equal to 10%, 6%, and 3% for occupancy categories I and II, III, and IV, respectively. A second basis is that life safety of occupants will be preserved in the design earthquake ground motion. Corresponding values of maximum probability of failure that could lead to endangerment of individual lives conditioned on the occurrence of MCE ground motion are equal to 25%, 15%, and 10% for occupancy categories I and II, III, and IV, respectively.

ASCE07-10 uses the same methodology as FEMA 450. This code categorizes buildings into four seismic use group based on the risk associated with unacceptable performance and limits the story drift ratio to 2.5%, 2.5%, 2.0% and 1.5% for seismic use group I, II, III, and IV, respectively,

for structures lower or equal four stories, which are exposed to the design earthquake ground motion.

2.4 AISI lateral design

According to AISI Lateral Design, calculation of loads, forces, and combinations of loads shall be in accordance with ASCE07-10 in United States and Mexico, NBCC in Canada, or other applicable building codes.

3. Damage description in experimental tests

When a strap-braced CFS wall is subjected to lateral forces (wind or earthquake forces), the response of the wall emerges as a wide range of damages, including plastic deformation of straps, net section failure of straps, tilting and pull-out of screws, bearing of the elements near the connections, especially near the corner connections, distortional buckling, and shear failure of screws. Accordingly, structural elements are divided into the primary and the secondary categories in order to specify the performance of which components should be prioritized to control the structural behavior. The purpose of this section is to recognize the failure modes and to investigate their effect on the performance of strap-braced CFS walls as the primary elements in seismic assessment.

In this study, the investigation of damage levels of CFS strap-braced buildings is carried out based on study of the experimental results. To serve this purpose, the different levels of damage are investigated from the first step of the experiments to collapse level. The results of the experiments carried out in the Structural Engineering Laboratory of the University of Queensland are considered as the main reference which is mainly because in these experiments all stages of loading are recorded and description of different damages and their drift levels are reported. In order to further clarify the specimens, framing details and their material properties are specified. The experimental program consisted of ten 2400 to 2400 mm full-scale specimens categorized in three types as shown in Table 2. All of the frames are constructed by C channels of $90 \times 36 \times 0.55$ mm components connected together by one rivet at each flange. A 30×0.75 mm flat strap or 25×1.0 mm perforated strap in one sides of the frame was implemented as bracing system. An array of #10-16 self-tapping screws has been used to connect straps to the wall panels. In order to prevent frame's corners from rigid rotation, all specimens are fixed in corners by means of $50 \times 50 \times 3$ mm angels and # 12-14 screws. More details of three different wall panels are presented in Table 1.

The first specimen of type I was A1, in which straps were connected to interior studs in conjunction with GB on one side and a vertical load equal to 45.7 kN was applied to the studs. In this specimen, straps were tensioned obviously in 4.5 mm of lateral displacement (0.187% Drift), equal to 9.5 kN lateral resistance, which in turn showed that straps did not act as the main lateral resistance components. Hysteresis curve of A1 (Fig. 1) illustrates the point clearly, where the high level of stiffness and lateral resistance, low ductility, and sudden failure of the wall in the first steps of experiment can be attributed to GB behavior which has played a prominent role in lateral resistance. Tilting of the screw at GB to stud flange connections are observed in 6 mm (0.25%) displacement. Finally, the wall lost all the racking resistance on account of distortional buckling of 2nd and 4th studs located under vertical loads and conveying strap loads and GBs separation from the middle studs in 24 mm (1.0%) displacement.

Table 1 General characteristics of the tested walls

Shape	Types	Specimen Name	Bracing system	Strap	Gypsum board thickness (mm)
/	I	A1,A2	XB*+GB**	Flat 30×0.75 mm/G300	10
		A3	XB	Flat 30×0.75 mm/G300	-
		D2	XB	Flat 30×0.75 mm/G300	-
/	II	C1	XB+GB+Bracket	Flat 30×0.75 mm/G300	10
		C2	XB+GB+Double Bracket	Perforated 25×1.0 mm/G300	10
		C3	XB+Bracket	Perforated 25×1.0 mm/G300	-
/	III	D1	XB	perforated 25×1.0 mm/G300	-
		E1	XB	Flat 30×0.75 mm/G300	-

* XB: X Strap Bracing; ** GB: Gypsum Board

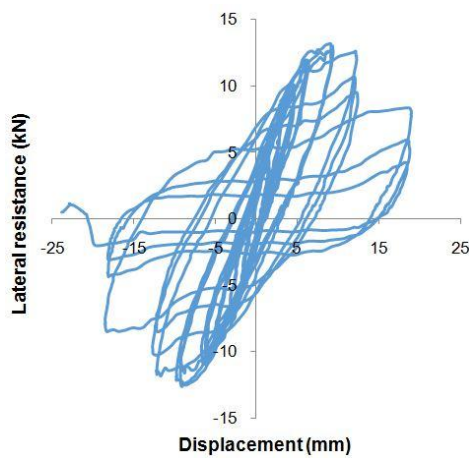


Fig. 1 Hysteretic curve of A1

The second specimen, A2, was similar to A1 in configuration and details but without vertical load. Damage report of this specimen is presented in Fig. 2.

The second type consisted of the walls in which four brackets were used in the corners. The first specimen was C1 in which straps were connected to both bracket flanges and frame corners. It was observed distortional buckling in the studs at 24 mm (1.0%) displacement. While the test was following the natural process, one of the straps suddenly tore in the bracket position through screws holes at 42 mm (1.75%) displacement, which primarily resulted from using three screws in limited space of the bracket flange. Thanks to the experience acquired from the previous specimen, C2 has equipped with double brackets to the corners.

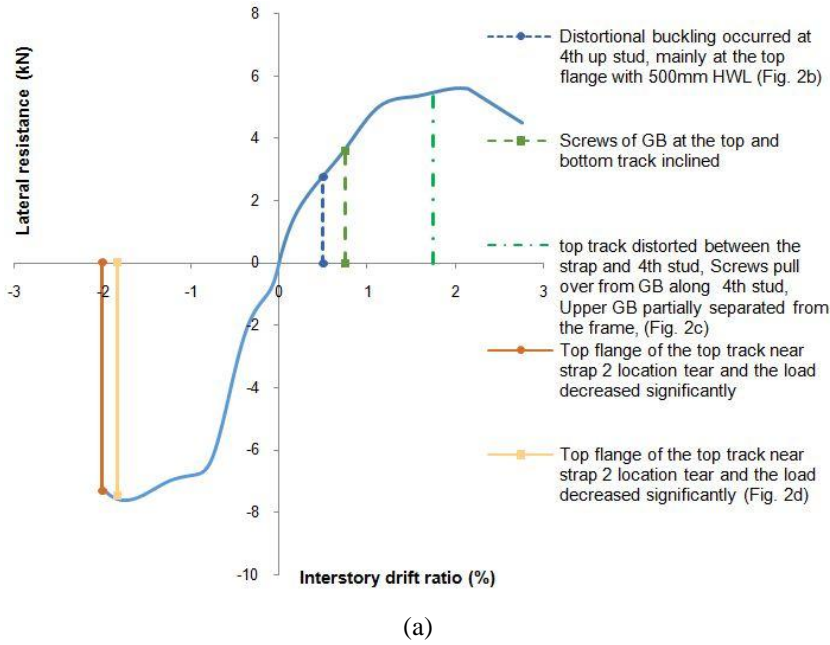


Fig. 2 Damage report of specimen A2



(b) Distortional buckling



(c) GB separation



(d) Tearing of the track

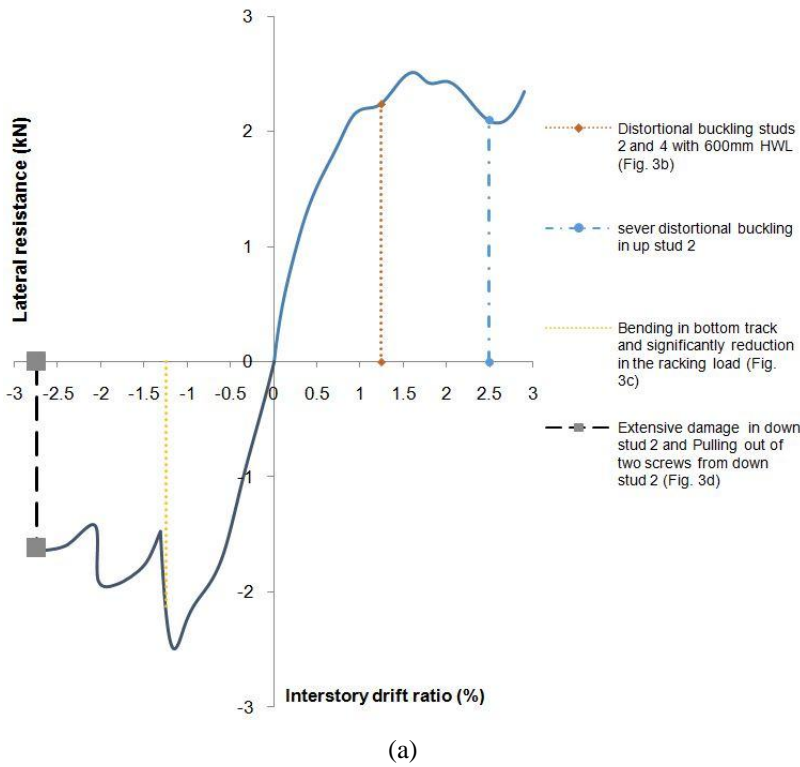


Fig. 3 Damage report of specimen A3



(b) Distortional buckling



(c) Severe distortional buckling



(d) Pulling out of the screws

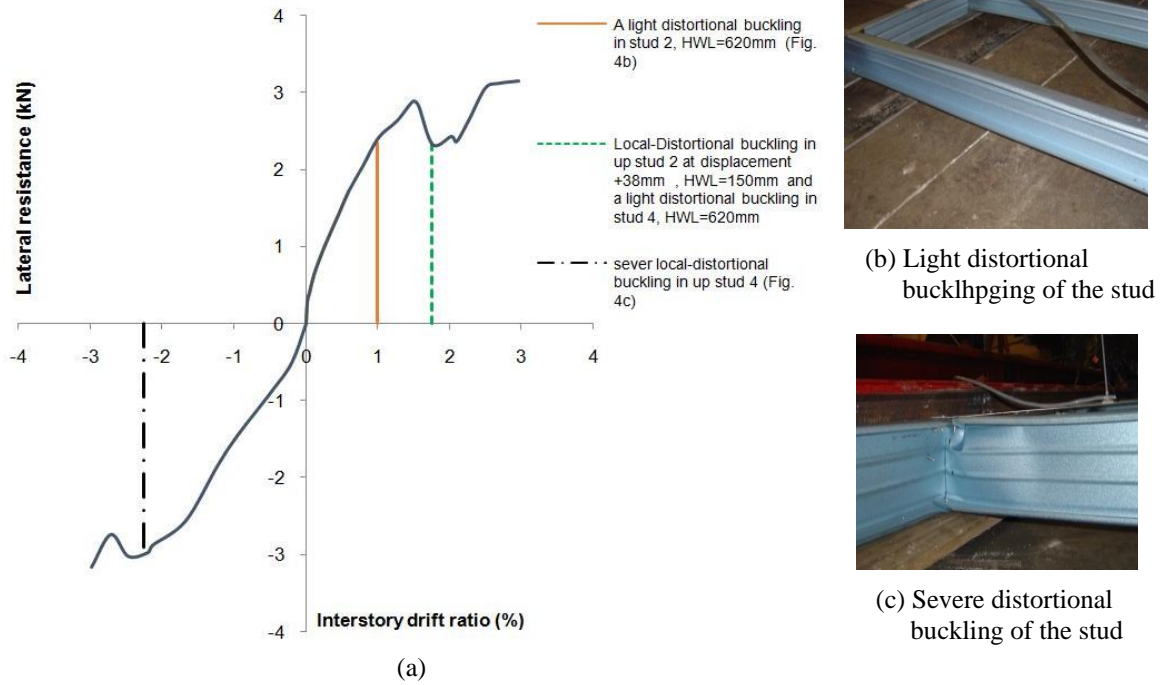


Fig. 4 Damage report of specimen D2

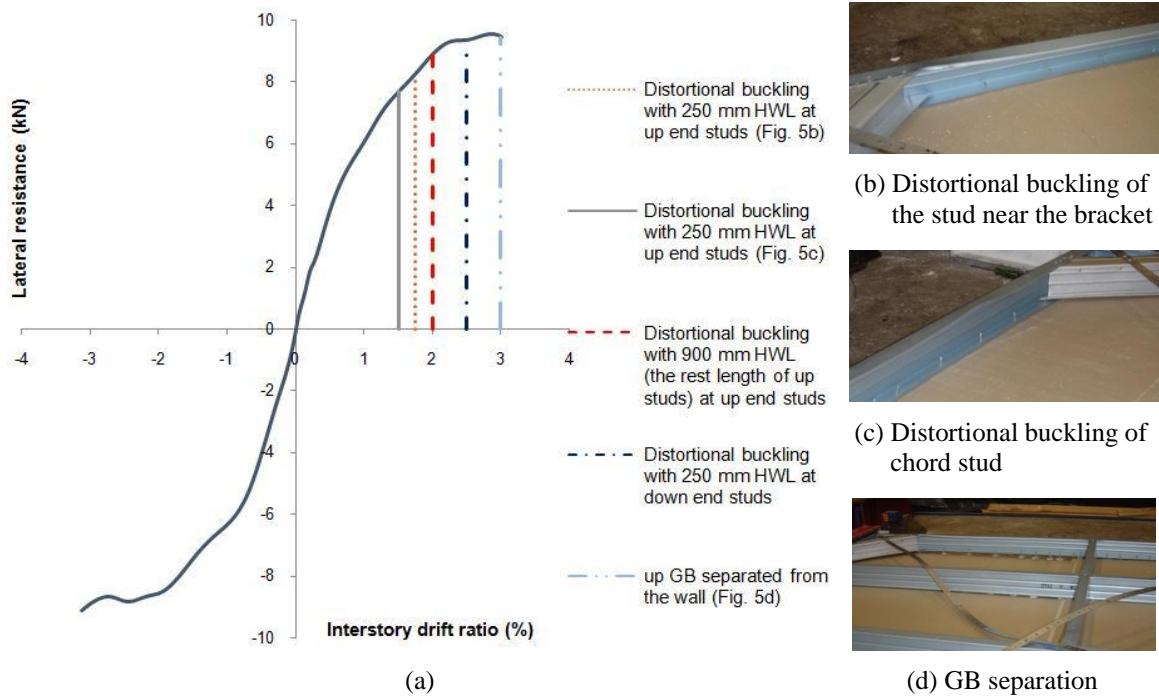
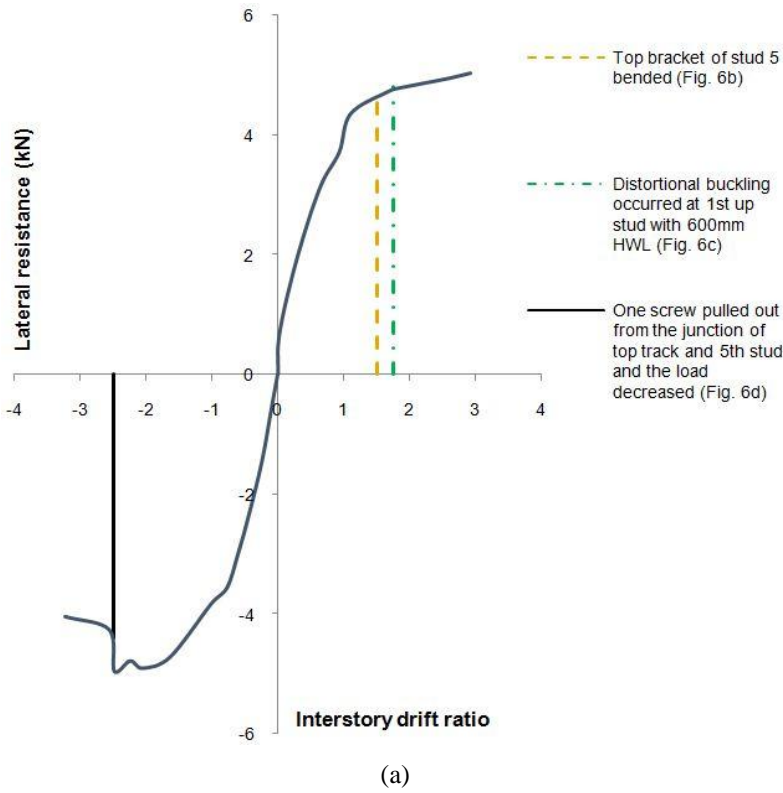
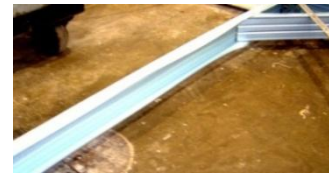


Fig. 5 Damage report of specimen C2



(b) Bending of the bracket

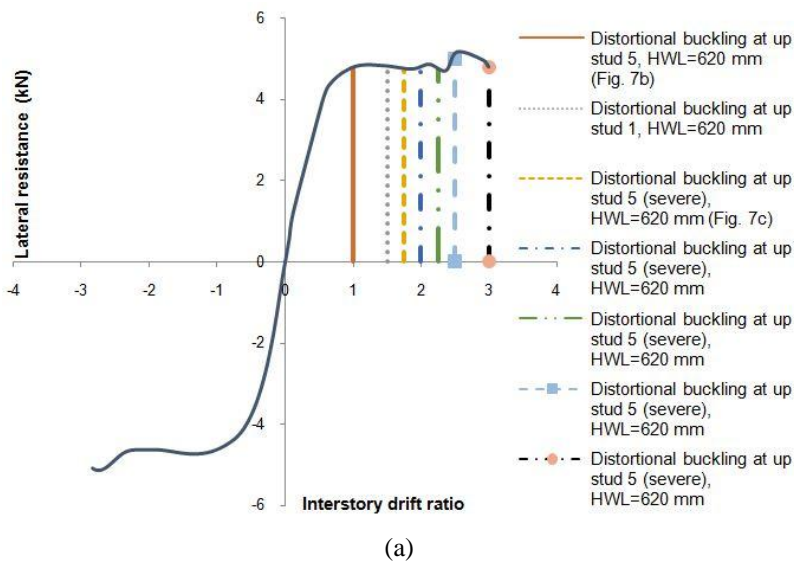


(c) Distortional buckling of chord stud



(d) Unsymmetrical bending of the bracket

Fig. 6 Damage report of specimen C3



(b) Distortional buckling of the stud



(c) Severe distortional buckling of chord stud

Fig. 7 Damage report of specimen E1

Last type of the frames consisted of two walls which had the same configuration with type I but straps have been connected to the chord flanges. Although specimen D1 had normal performance up to lateral displacement of 24 mm (1.0%) in which some sort of distortional buckling occurred in the chords, the wall underwent serious damages at only 30 mm (1.25%) displacement. This was mainly because the chords and their connections were not strong enough to convey the lateral load.

The investigation of other researches reveals that there are similar events which cause serious damages to the walls. In these experiments, researchers mostly focused their attention on the considerable structural damages which result in structural collapse. Here, some of these researches are reviewed with the aim of finding damage processes.

Fulop and Dubina (2008) tested two strap-braced frames under uniform and cyclic loading. They observed local deformations of the lower tracks at the beginning of the experiments. By increasing lateral displacement, damages concentrated entirely in corners. Following the concentration of damage to corners, some signs of connection elongation, and redistribution of load to the interior studs and important plastic elongation of the straps were observed. Ultimately, with the buckling of the chord elements and connection failure, the test was stopped. Investigation of the hysteresis curves shows that buckling of the chord elements which have resulted in a considerable decrease in lateral resistance have occurred in the 2.5% of drift, approximately.

Al-kharat and Rogers (2007) conducted their experiments on strap-braced light steel frames in three categories based on lateral load capacity of light (20 kN), medium (40 kN) and heavy (75 kN). They observed strap yielding combined with serious bearing of track and chord to stud connections. Moreover, strap yielding has been observed in all medium frames in which hold-down had installed in corners. Serious distortional buckling in the chord to hold down joints is occurred in the range of 2.5% to 3.0% of drift ratio. Also, net section failure of strap occurred after a range of 3.0% of drift ratio. This is noticeable that the damages happened to medium walls are similar to those observed by Fulop and Dubina (2008).

Moghimi and Ronagh (2009a) reported a wide variety of the damages such as hairline cracks of gypsum board gladding, screws tilting, bearing of gladding corners, and weak buckling of studs in the first steps of their tests. Severe distortional buckling of studs and bearing of the wing of tracks in neighborhood of the joints occurred at drift 1.0% to 1.75%. Also, pulling over of gladding (gypsum board), tearing of the track wing in the strap to frame connections, and serious distortional buckling of the chords were reported in the range of 2.25% to 3.0% of drift.

4. Seismic performance levels

Investigations of the experimental results show that it is possible to categorize damages into three seismic performance levels, as follow:

a. Immediate Occupancy (IO) performance level, in which the damages are negligible and the performance of structures is elastic. In the strap-braced CFS frames, it is possible to express that the strap-braced frames which are sheathed with GB have experienced negligible bearing of gypsum boards and tilting of screws during the first steps of experiment at 0.25% to 0.3% of drift. Therefore, IO performance level is equivalent to hairline cracks in the gladding and negligible tilting of screws. The allowable drift limitation of IO performance level employed is 0.3%.

b. Life Safety (LS) performance level, in which a wide range of damage such as bearing of track wing in some connections, strap yielding, local bearing and pulling over of GB, severe screws tilting, and distortional buckling of studs happen. Distortional buckling in chords with half

wave length (HWL) of 500 and 1000 mm and negligible local buckling at studs and tracks have started from the range of 0.5% to 0.75% of drift. Moreover, significant tilting of the screws at strap to frame connection in some joints and partially separation of gypsum board to studs connections occurred in the range of 1.0% to 1.75% of drift. The allowable drift limit of LS performance level is 1.75%.

c. Collapse Prevention (CP) performance level, in which the walls can expose to very severe damages such as connection fracture, net section failure of the straps or high level of strap yielding, and severe distortional buckling of the chords. Since the drift ratio has exceeded 1.75%, damages concentrate at corners and stability of the frames challenges by a wide range of damages, e.g., gladding to frame connection fully separation, severe distortional buckling of track to stud connections, pulling out of the screws at the strap to frame connections, which in turn results in tearing of strap and components, severe distortional buckling of studs, strap yielding and net section failure of strap in some samples up to the drift ratio of 2.5% to 3.0%. The allowable drift limitation of CP performance level employed is 2.5%.

5. Performance assessment

When a structure is constructed, one of the most important question is that how this structure reacts against different earthquakes. Seismic performance investigation may be an effective solution to answer this question. In order to assess seismic performance, it is required to make an analytical model which operates as a real full-scale specimen. Admittedly, each analytical model needs to have structural parameters and details. To this end, a series of frames consisted of 8 full-scale specimens categorized in three types as shown in table 2 are selected. Four specimens including DA2, DA3, CC1, and CD1 are selected from Moghimi and Ronagh (2009a) research. All of the frame components, i.e. top and bottom tracks, noggins and studs, were identical to those of used in this paper's experimental program. More details can be found in the reference (Moghimi and Ronagh 2009a). In order to assess the seismic performance of the strap-braced CFS walls, each wall was modeled as a single degree of freedom system.

5.1 Analytical model

When a strap-braced stud wall undergoes the lateral loading, the path of load transmission is from strap to chord and from their joint to anchorage system. Hence, total frame stiffness is a combination of strap stiffness, studs and anchorage system stiffness in which strap plays an essential role in total stiffness of the system up to the point that strap yielding contributes to global yielding of the wall.

Experimental studies on strap-braced stud walls revealed that pinching of hysteretic curve and stiffness degradation are two most common events which affect hysteresis lateral behavior. Stiffness degradation can primarily contribute to strap yielding and pinching in hysteretic curve results from the inability of straps to carry compression force. Consequently, as a tension-only strap enters the inelastic region, the lateral loading of the frame starts from the last loop of hysteresis curve that the frame has experienced. In other words, plastic deformation of strap and negligible effect of other elements in lateral stiffness cause a rigid displacement of wall in each cycle of loading. Fig. 8 shows hysteresis curve of E1 specimen that is a clear-cut example in which plastic deformation (Δ_{plastic}) and rigid motion are obviously happened.

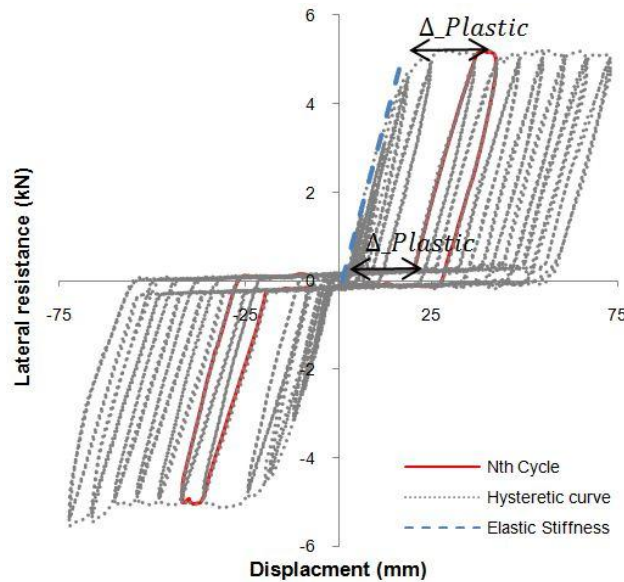


Fig. 8 Hysteresis behavior of E1 specimen

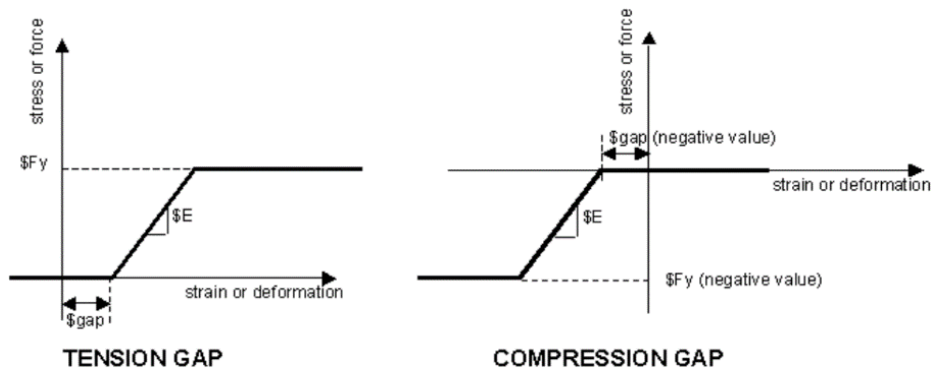


Fig. 9 Elastic-Perfectly Plastic Gap Material (OPENSEES)

In order to provide a hysteretic model of the strap-braced stud wall, which considers rigid motion and stiffness degradation, Elastic-Perfectly Plastic Gap Material, as implemented in OPENSEES (Mazzoni *et al.* 2007), is pursued. Elastic-Perfectly Plastic Gap Material parameters includes tangent stiffness (E), yielding stress or force (F_y), initial gap (strain or deformation), and second stiffness, as shown in Fig. 9. Moreover, Elastic-Perfectly Plastic Gap Material has offered an option which considers accumulative damage. Regarding a strap-braced stud wall as a single degree of freedom system, a feasible solution in order to accurately model the stiffness parameter of the wall is to pursue a spring or element with Elastic-Perfectly Plastic Gap Material's behavior.

5.2 Stiffness calculation

The stiffness parameters have been calculated according to FEMA 356 in which the general

Table 2 Stiffness parameters obtained by FEMA-356 method

Type	Frame	δ_t (mm)	V_t (kN)	δ_y (mm)	V_y (kN)	K_e (kN/mm)	α
I	E1	60	5.07	16.84	4.97	0.30	0.01
	DA3	60	4.32	8.06	3.58	0.44	0.03
	DA2	60	4.40	10.55	3.44	0.33	0.06
II	C3	60	4.64	9.58	3.82	0.40	0.04
	CC1	60	4.58	21.41	4.19	0.19	0.05
	CD1	60	9.35	19.75	6.38	0.32	0.07
III	A2	60	6.03	8.46	5.15	0.61	0.02
	C2	60	9.31	19.9	6.67	0.34	0.07

* δ_t : Target displacement; δ_y : Yield displacement

** V_t : Target strength; V_y : Effective yield strength

*** K_e : Effective lateral stiffness

**** α : Post-yield slope

structural response of the structure has been equalized with a bilinear curve so that the size of the areas above and below of the curve shall be balanced and the initial secant stiffness shall be calculated using a base shear force equal to 60% of the idealized yield strength of the structure. The second segment line and the post-yield slope shall be determined by a line passing through the actual curve at the calculated target displacement. In this study, it is assumed that the target displacement is allowable in story displacement associated to the CP seismic performance level. Table 2 presents the stiffness parameters of the frames.

5.3 Mass calculation

A rational hypothesis is required to calculate the maximum load (mass) which can be supported by the frames. Hence, it is assumed that in all frames, failure mode is strap yielding and all components and joints do not receive any failure up to the point of strap yielding.

In order to estimate the mass, the demand and the capacity of the structure should be calculated. On the one hand, the demand is calculated exploiting ASCE7-10 standard in which strength reduction factor of 0.9 has been assigned for tensile members. In addition, regarding the fact that straps have no role in the gravity loading, the earthquake load coefficient of 1.0 is considered. Also, equivalent linear static analysis was utilized in which the response modification factor of 4.0 is assigned for strap-braced CFS stud walls in order to calculate maximum base shear force coefficient. It is assumed that the building occupancy is residential (risk category II), soil category is C, and mapped acceleration parameters, S_s and S_1 are considered 0.5, 0.15 respectively.

On the other hand, the seismic capacity of the structure is calculated using shear force, V_s , from experimental push curves. According to investigation performed on the ANSYS (2009)'s outputs, the significant overall yielding of the structure, V_s , equates with the point where the deviation of lateral response of the structure from the linear trend-line which fitted on linear part of the envelope curve be equal to 0.5%. Fig. 10 shows the significant overall yielding of the DA2 specimen, graphically. The drifts' deviation is calculated using Eq. (1). For this purpose, the curve's nodes which have drifts of up to %10 of the maximum shear wall's drift, $d_{c,max}$, were considered

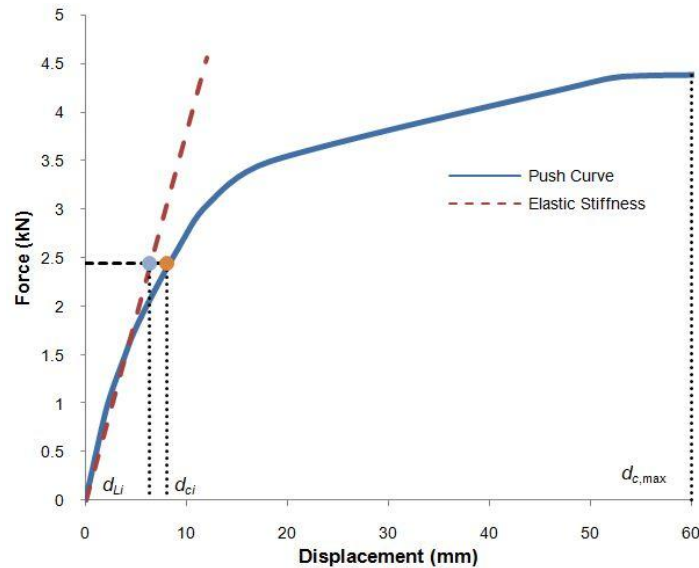


Fig. 10 Calculation of the drifts' deviations of DA2 specimen

$$D_i = (d_{Li} - d_{ci})/d_{c,max} \quad (\%) \tag{1}$$

Where D_i is the drifts' deviations associated with the i^{th} point (X_i); d_{Li} is the drift of linear trend-line associated to point X_i ; d_{ci} is the drift of the envelope curve associated to point X_i ; and $d_{c,max}$ is the Maximum shear wall's drift (ANSYS 2009).

The mass is calculated with regard to the present assumptions and the maximum lateral strength. For example, calculating of the maximum sustainable mass of DA2 frame is presented:

$$S_S = 0.5 \text{ g}, S_1 = 0.15 \text{ g}, \text{ site class} = C, \text{ and seismic use group} = \text{II}; F_a = 1.2, R = 4.0, I_e = 1.0$$

$$S_{MS} = F_a S_S = 1.2 \times 0.5 = 0.6; S_{DS} = \frac{2}{3} S_{MS} = \frac{2}{3} \times 0.6 = 0.4;$$

$$C_S = \frac{S_{DS}}{\left(\frac{R}{I_e}\right)} = \frac{0.4}{\left(\frac{4}{1}\right)} = 0.1; V_E = C_S W = 0.1 \times mg$$

Because of the failure mode of the frames is selected as strap yielding, the strength reduction factor (ϕ), 0.9 is considered. Due to an inability of straps on the compression loads bearing, only earthquake load is considered in the demand (D) calculations.

$$D = 1.0 \times V_E = 0.1 \times mg$$

As previously mentioned, capacity (C) of the frames are calculated from experimental pushover curves. For DA2 frame, $V_S(C)$ is calculated equal to 2.436 kN.

$$\phi C = 0.9 \times 2436 = 2192 \text{ N}; \quad 0.1 \times mg \leq 2192; \quad m \leq 2235 \text{ Kg}$$

The obtained masses of all specimens are presented in Table 3.

Table 3 Maximum allowable mass

Type	Frame	V_s (kN)	Mass (kg)
I	EA1	2.58	2364
	DA3	2.50	2297
	DA2	2.44	2235
II	C3	2.75	2521
	CC1	2.16	1980
	CD1	2.13	1955
III	A2	3.94	3615
	C2	3.28	3016

5.4 Damping

According to the experimental results obtained by Kim *et al.* (2006), damping ratio of strap brace stud wall was estimated to be 7.2%. Fulup and Dubina (2004) used 5% damping ratio to evaluate dynamic response of numerical modeling of strap bracing frames. In this paper, the viscous damping ratio has been set equal to 5.0%.

5.5 Model verification

To verify this model, these parameters are calculated for two hysteresis diagrams. Corresponding frames were modeled in the OPENSEES program. The hysteresis diagram from cyclic analysis of these models is compared with the experimental tested diagram. Fig. 11 shows experimental data fitting for the procedure used as in prior relations. Analytically calculated cyclic diagrams and a comparison between analytical and experimental tested diagrams are represented in the left and right-hand side diagrams, respectively.

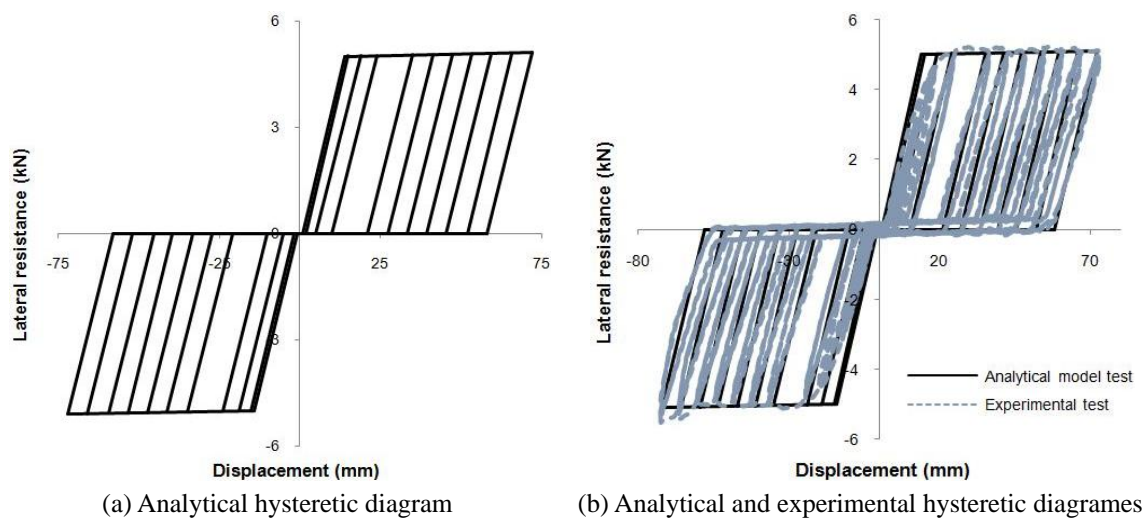


Fig. 11 Comparison between analytical and experimental tested diagram of E1 specimen

6. Incremental dynamic analysis

Incremental Dynamic Analysis (IDA) is a parametric analysis method that involves subjecting a structural model to one or more ground motion record(s) scaled to multiple levels of intensity. In order to perform the IDA procedure, a Number of ground motion records should be selected. Shome and Cornell (1999) have shown that for mid-rise buildings, ten to twenty records are usually enough to adequately cover the range of magnitude and distance of ground motions. In this study, a set of fourteen ground motion records is selected, listed in Table 4, that have magnitude ranges of 6.5-6.9 and moderate distances. For performing an IDA, the Intensity Measure (IM) and Damage Measure (DM) are selected as peak ground acceleration (PGA) and maximum inter-story drift ratio, respectively.

7. Performance assessment using fragility curves

Seismic fragility function is a mathematical expression which indicates the conditional probability that a component or system will experience damage equal to or more severe than a particular level, given that it experiences earthquake-induced demands of a particular severity. In simpler terms, the fragility defines the conditional probability of the Earthquake Demand Parameter (EDP) placed upon the structure exceeding its Limit State (L.S.) capacity for a given level of ground motion intensity (IM), as shown in the Eq. (2).

$$\text{Fragility} = P [\text{EDP} \geq \text{L.S.} \mid \text{IM}] = 1 - P [\text{EDP} < \text{L.S.} \mid \text{IM}] \quad (2)$$

The formulation presented above illustrates the fragility for representative element and demand parameter. By considering the lognormal distribution, fragility function derives as Eq. (3).

Table 4 Selected Records for IDA (Shome N., Cornell CA. 1999)

No.	Event	Station	PGA (g)
1	Loma Prieta 1989	Agnews State Hospital	0.159
2	Imperial Valley 1979	Plaster City	0.057
3	Loma Prieta 1989	Hollister Diff. Array	0.279
4	Loma Prieta 1989	Anderson Dam Downstream	0.244
5	Loma Prieta 1989	Coyote Lake Dam Downstream	0.179
6	Loma Prieta 1989	Sunnyvale Colton Ave	0.207
7	Imperial Valley 1979	El Centro Array #13	0.117
8	Loma Prieta 1989	Hollister South & pine	0.371
9	Loma Prieta 1989	Sunnyvale Colton Ave	0.209
10	Superstition Hills 1987	Wildlife Liquefaction Array	0.18
11	Imperial Valley 1979	Chihuahua	0.254
12	Imperial Valley 1979	Westmorland Fire Station	0.11
13	Imperial Valley 1979	Plaster City	0.042
14	Loma Prieta 1989	Hollister Diff. Array	0.269

$$\text{Fragility} = 1 - \Phi\left(\frac{\ln(L.S.) - \lambda}{\sqrt{\beta_1^2 + \beta_2^2 + \dots + \beta_n^2}}\right) \quad (3)$$

Where, Φ is the standard lognormal Gaussian cumulative distribution function, λ is logarithm of median of the maximum response and β_i ($i = 1, 2, \dots, n$) represent various uncertainties.

Many sources of uncertainty contribute to variability in collapse capacity. It is important to evaluate all significant sources of uncertainty in collapse response, and to incorporate their effects in the seismic assessment process. According to FEMA-P695, the sources of uncertainty are composed of 4 parameters, as Eq. (4).

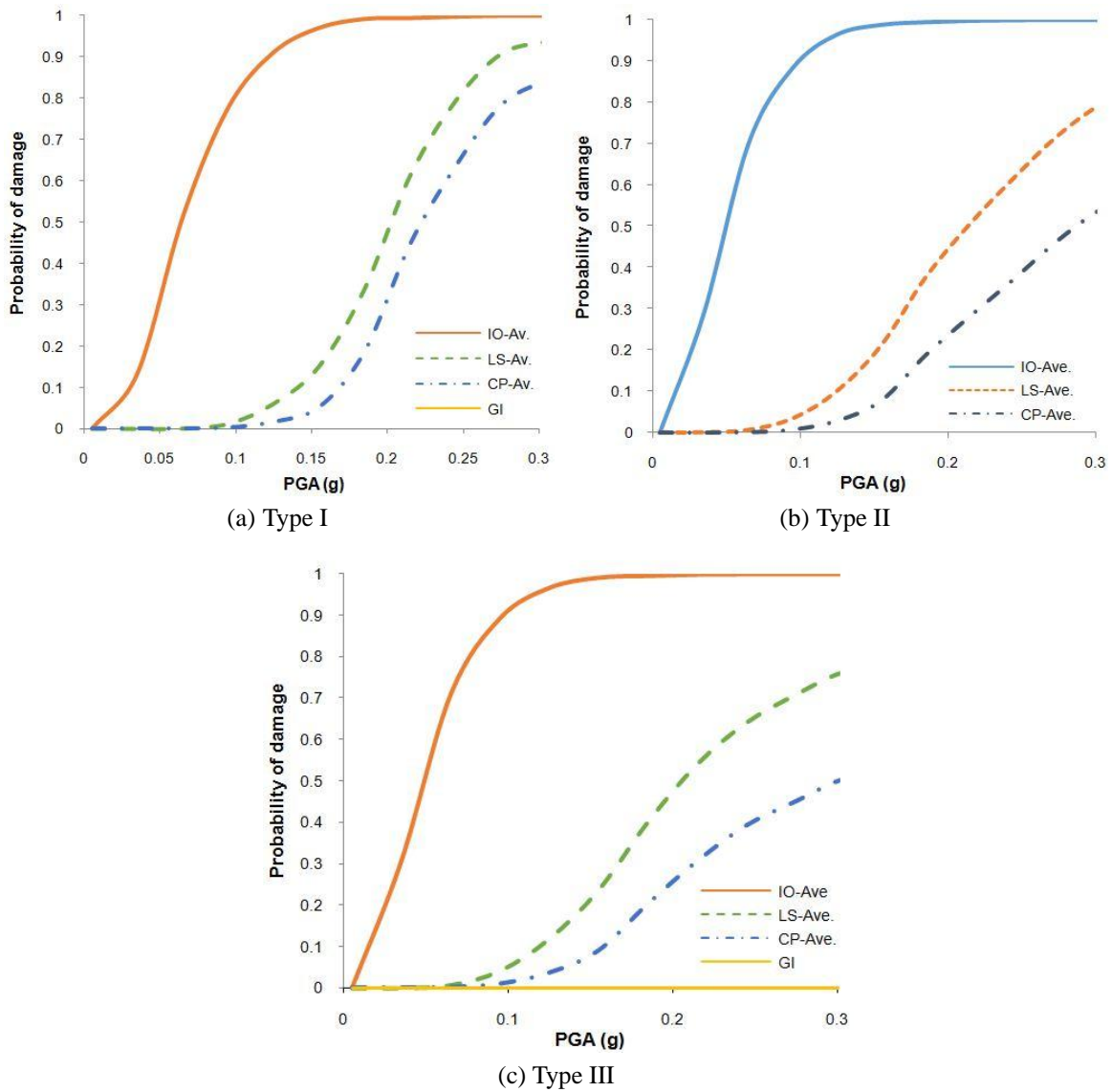


Fig. 12 Average fragility curves

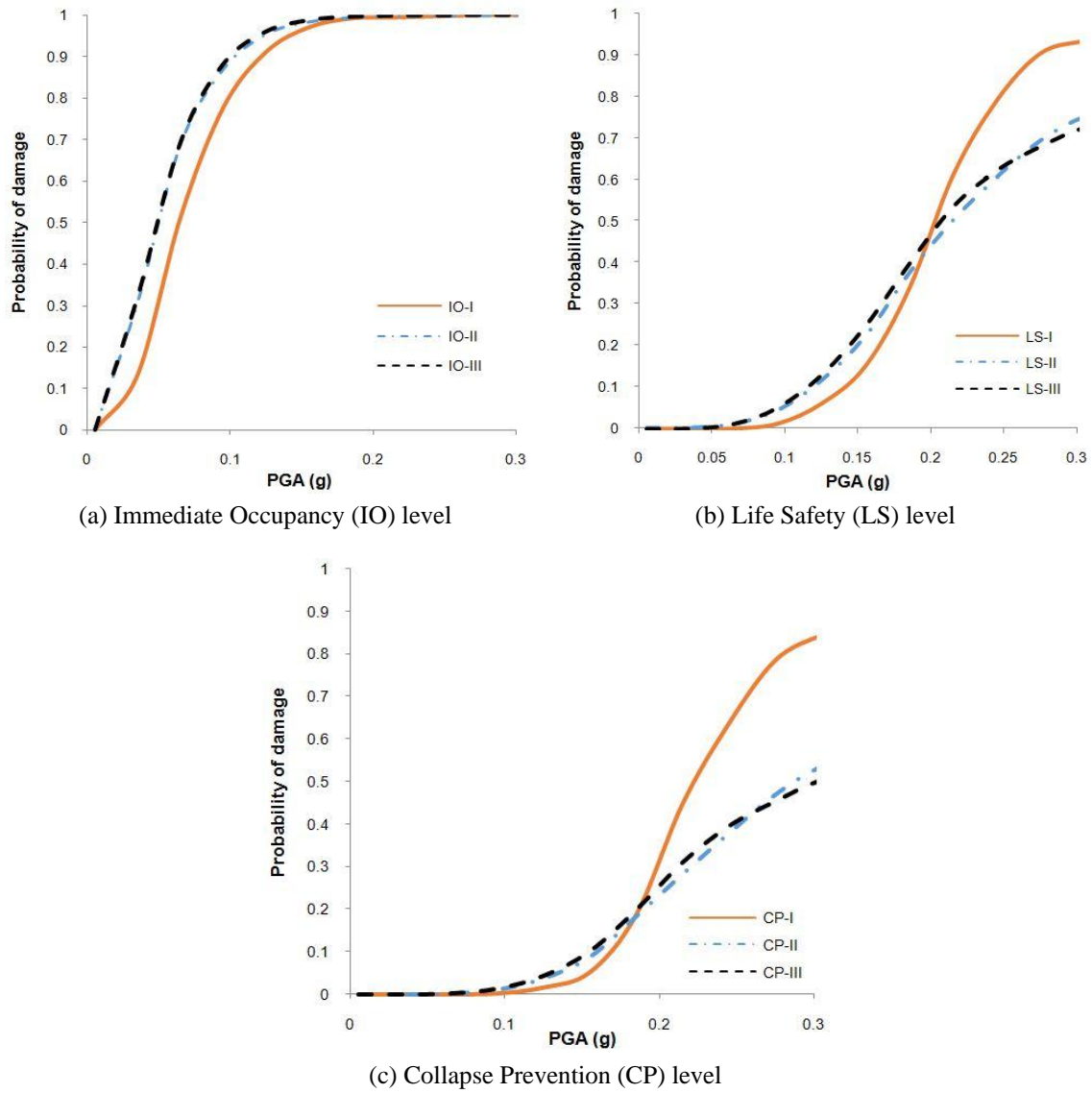


Fig. 13 Comparative fragility curves of types I, II and III

$$\beta_{TOT} = \sqrt{\beta_{RTR}^2 + \beta_{DR}^2 + \beta_{TD}^2 + \beta_{MDL}^2} \tag{4}$$

Where, β_{RTR} is the record-to-record collapse uncertainty, β_{DR} is uncertainty of the seismic capacity due to design requirements. β_{TD} is uncertainty of the seismic capacity due to test data. β_{MDL} is uncertainty of the structural modeling due to dispersion of modeling parameters. Based on FEMA-P695, β_{DR} , β_{TD} and β_{MDL} are calculated 0.2, 0.2 and 0.35, respectively.

Fig. 12 shows the average fragility curves of three types of the strap-braced CFS walls presented in Table 1. The x -axis represents the Peak Ground Acceleration (PGA) and y -axes

represent Cumulative Probability Function (CPF). The IO-fragility curves show that all specimens will experience a series of damage associated with the IO seismic performance level if the earthquakes with 0.2 g of PGA happen. However, seismic behavior of three types for LS and CP performance levels differ significantly. For example, compare LS-fragility curve of type I with that of type III. Results show that there is 85% probability that an earthquake with 0.3 g of PGA results in excessive damage up to CP limit state to type I, but there is a 50% probability that cladding walls (type III) experience the CP limit state if the earthquakes with 0.3 g of PGA happen. In addition, in the case of the type II and III, it can be observed that the difference between the probability of LS and CP damage levels have increased while PGA of earthquake increases, which in turn shows the major impact of strong earthquakes on the probability of exceeding the LS damage level. In the meanwhile, in the case of the type I, there is no obvious deference between the probability of LS and CP damage levels. This is mainly because of elastic-perfectly plastic behavior of the walls.

Comparative Figures (Fig. 13) for three types of the strap-braced CFS walls clearly show the effective influence of the bracket and cladding on the decrease of probability of exceeding the LS and CP damage levels. Fig. 13 shows the similar results of type I and II, which mainly results from positive effect of the cladding and bracket on the stiffness, especially post-yielding stiffness of the specimens.

Furthermore, the seismic performance of strap-braced CFS stud walls can be assessed by investigation of the maximum probability of failure offered by ASCE07-10. In this study it is assumed that the frames are classified as Seismic category II with soil site class C. Accordingly, PGA of maximum considered earthquake and PGA of design earthquake ground motion are estimated 0.28 g and 0.20 g, respectively. As can be seen in Figs. 11(a)-(c), in the PGA associated with the maximum considered earthquake (MCE) ground motion, the probability of exceeding the IO damage level of all the three types is 100% and the probability of exceeding the LS damage level of type I, II and III is 90%, 72% and 70%, respectively. Also, the probability of collapse of type I, II and III is 80%, 45% and 42%, respectively. Meanwhile, ASCE07-10 considers maximum probability of failure that could lead to endangerment of individual lives and total or partial structural collapse equal to 25% and 10%, respectively.

From seismic performance objective perspective, based on FEMA P750, the expected performance of ordinary buildings (seismic use group II) is to remain in IO seismic performance level at the frequent ground motion and stay in LS seismic performance domain at the design ground motion and finally collapse under MCE ground motion. Figs. 11(a)-(b) show that all three types of strap-braced CFS stud walls will experience LS level with the probability of 99% and will collapse with the probability of 45%.

8. Conclusions

The two main purposes of this paper are to recognize all damages which may happen during seismic events so as to define seismic performance levels of strap-braced stud walls and to assess their seismic performance during and after seismic events, which result in important conclusions as:

- The most serious damages of the strap-braced CFS walls are concentrated in the connections, especially straps to frame connections. Therefore, the use of anchorage system, gusset plate, and bracket in corners set the stage for optimal performance of the walls.

- Based on FEMA 356, seismic performance levels of strap-braced CFS stud walls should be defined as same as *x*-braced hot-rolled steel structures. But, the yielding point of strap-braced CFS walls associates with a number of considerable damages which may endanger the Immediate Occupancy level of these systems. Also, experiments have shown that some of failure modes of the strap-braced CFS walls are substantially different from those of hot-rolled steel structures which have been characterized by plastic deformation of their elements.
- In the case of the X brace-only CFS walls, the lateral stiffness and strength of the walls are mainly influenced by strap properties up to the point that yielding of the wall and strap almost happens simultaneously. Moreover, the post-yielding behavior of these walls obeys the post-yielding behavior of the strap.
- Although strap yielding is immensely influential in seismic performance of the strap-braced CFS walls, a wide range of damages such as strap tearing, pulling out of screws, or severe distortional buckling of studs may be happened and consequently the CFS walls pass the immediate occupancy level and close to collapse. Therefore, it seems that considering the strap yielding as the only mode of failure of the strap-braced CFS walls is not logical.
- The outcomes of the probabilistic analysis of the strap-braced CFS walls indicate that relying solely on the strap stiffness and strength for attaining the acceptable seismic performance do not have a quite satisfactory outcome.
- The utilization of lateral stiffness and strength of the cladding and bracket can be very beneficial to significantly decrease the probability of occurrence of damages.

Acknowledgments

Special thanks for his contributions throughout the experimental project goes to Prof. H.R. Ronagh.

References

- AISI S213-07 (2007), North American Standard for Cold -Formed Steel Framing – Lateral Design; American Iron and Steel Institute, Washington D.C., USA.
- Al-Kharat, M. and Rogers, C.A. (2007), “Inelastic performance of cold-formed steel strap braced walls”, *J. Construct. Steel Res.*, **63**(4), 460-474.
- ANSYS (2009), I. ANSYS 12.0.1 — User’s manual.
- ASCE/SEI 7-10 (2010), Minimum design loads for buildings and other structures; American Society of Civil Engineers, Reston, VA, USA.
- Casafont, M., Arnedo, A., Roure, F. and Rodriguez-Ferranon, A. (2006a), “Experimental testing of joints for seismic design of lightweight structures. Part 1. Screwed joints in straps”, *Thin-Wall. Struct.*, **44**(2), 197-210.
- Casafont, M., Arnedo, A., Roure, F. and Rodriguez-Ferranon, A. (2006b), “Experimental testing of joints for seismic design of lightweight structures. Part 2: Bolted joints in straps”, *Thin-Wall. Struct.*, **44**(6), 677-691.
- Casafont, M., Arnedo, A., Roure, F. and Rodriguez-Ferranon, A. (2007), “Experimental testing of joints for seismic design of lightweight structures. Part 3: Gussets, corner joints, x-braced frames”, *Thin-Wall. Struct.*, **45**, 637-659.
- Dubina, D. (2008), “Behavior and performance of cold-formed steel-framed houses under seismic action”, *J. Construct. Steel Res.*, **64**, 896-913.

- FEMA P695 (2008), Quantification of Building Seismic Performance Factors, Prepared by the Building Seismic Safety Council for the Federal Emergency Management Agency; Federal Emergency Management Agency, Washington D.C., USA.
- FEMA P750 (2009), NEHRP recommended seismic provisions for new buildings and other structures; Federal Emergency Management Agency, Washington D.C., USA.
- FEMA 356 (2002), NEHRP guidelines for the seismic rehabilitation of buildings; Federal Emergency Management Agency, Washington D.C., USA.
- FEMA 450 (2003), NEHRP recommended provision for seismic regulations for new buildings and other structures; Federal Emergency Management Agency, Washington D.C., USA.
- Fulop, L.A. and Dubina, D. (2004), "Performance of wall-stud cold-formed shear panels under monotonic and cyclic loading Part II: Numerical modeling and performance analysis", *Thin-Wall. Struct.*, **42**(2), 339-349.
- Ghowzi, A.F. and Sahoo, D.R. (2015), "Fragility assessment of buckling-restrained braced frames under near-field earthquakes", *Steel Compos. Struct., Int. J.*, **19**(1), 173-190.
- Hatami, S., Ronagh, H.R. and Azhari, M. (2008), "Behaviour of thin strap-braced cold-formed steel frames under cyclic loads", *Proceedings of the 5th International Conference on Thin-Walled Structures*, Brisbane, Australia, June.
- Iuorio, O., Macillo, V., Teresa Terracciano, M., Pali, T., Fiorino, L. and Landolfo, R. (2014), "Seismic response of CFS strap-braced stud walls: Experimental investigation", *Thin-Wall. Struct.*, **85**, 466-480.
- Karantoni, F., Tsionis, G., Lyranzaki, F. and Fardis, M.N. (2014), "Seismic fragility of regular masonry buildings for in-plane and out-of-plane failure", *Earthq. Struct.*, **6**(6), 689-713.
- Khaloo, A., Nozhati, S., Masoomi, H. and Faghihmaleki, H. (2016), "Influence of earthquake record truncation on fragility curves of RC frames with different damage indices", *J. Build. Eng.*, **7**, 23-30.
- Kiani, A., Mansouri, B. and Moghadam, A.S. (2016), "Fragility curves for typical steel frames with semi-rigid saddle connections", *J. Construct. Steel Res.*, **118**, 231-242.
- Kim, T.W., Wilcoski, J., Foutch, D.A. and Lee, M.S. (2006), "Shaketable tests of a cold-formed steel shear panel", *Eng. Struct.*, **28**(10), 1462-1470.
- Mazzoni, S., McKenna, F., Scott, M.H., Fenves, G.L. *et al.* (2007), OPENSEES Command Language Manual, Department of Civil Environmental Engineering, University of California, Berkeley, CA, USA.
- Moghimi, H. and Ronagh, H.R. (2009a), "Performance of light-gauge cold-formed steel strap-braced stud walls subjected to cyclic loading", *Eng. Struct.*, **31**(1), 69-83.
- Moghimi, H. and Ronagh, H.R. (2009b), "Better connection details for strap-braced CFS stud walls in seismic regions", *Thin-Wall. Struct.*, **47**(2), 122-135.
- NBCC (2005), National Building Code of Canada, Ottawa, Canada.
- Shome, N. and Cornell, C.A. (1999), "Probabilistic seismic demand analysis of nonlinear structures", Report No. RMS-35; RMS Program, Stanford University, Stanford, CA, USA.
- Velchev, K., Comeau, G., Balh, N. and Rogers, C.A. (2010), "Evaluation of the AISI S213 seismic design procedures through testing of strap braced cold-formed steel walls", *Thin-Wall. Struct.*, **48**(10-11), 846-856.